Materials Research Bulletin 115 (2019) 196–200

Contents lists available at ScienceDirect

Materials Research Bulletin

journal homepage: www.elsevier.com/locate/matresbu

Temperature-dependent photoluminescence characterization of compressively strained AlGaInAs quantum wells

Yue Song[a,b], Ligong Zhang[a,*], Yugang Zeng[a,*], Yongyi Chen[a], Li Qin[a], Yinli Zhou[a], Yongshi Luo[a], Haifeng Zhao[a], Yongqiang Ning[a], Lijun Wang[a]

[a] State Key Laboratory of Luminescence and Applications, Changchun Institute of Optics, Fine Mechanics and Physics, Chinese Academy of Sciences, Changchun 130033, China

[b] University of Chinese Academy of Sciences, Beijing, 100049, China

ARTICLE INFO

Keywords:
A. $Al_{0.07}Ga_{0.22}In_{0.71}As$ quantum wells
B. Optical properties
B. Metal organic chemical vapor deposition
C. Photoluminescence
D. Full width at half maximum

ABSTRACT

A series of compressively strained AlGaInAs quantum well (QW) structures with different annealing treatment durations at 170 °C were investigated by temperature-dependent photoluminescence (PL). An abnormal S-shaped behavior in emission energy and a non-monotone evolution in spectral band width were observed at low temperature. A significant negative linear correlation between full width at half maximum (FWHM) and emission energy at different test temperature was exhibited in samples with different heat treatment durations. The highly linear relation demonstrated that the dependencies and relationships between PL peak energy and FWHM vs temperature are consistent. The anomalous blue shift and concomitant narrowing of FWHM in AlGaInAs QW were affected by lattice strain fluctuations due to the difference of thermal expansion coefficients between adjacent layers and strong carriers' localization at low temperature.

1. Introduction

The AlGaInAs material system is a good candidate for the active layer of semiconductor diode lasers emitting wavelengths at 1310 nm and 1550 nm owing to some incomparable characteristics, such as low threshold current density and high modulation speed [1,2]. Their structural and optical properties have been widely investigated in the past few decades [3–5]. An atypical band gap energy shift characteristic was observed in compressively strained quaternary AlGaInAs quantum well (QW) at low temperature [6], which was similar to the temperature-induced S-shaped PL shift observed in many ternary III-V compound semiconductor materials [7,8]. However, an agreement has not been reached yet by researchers on the mechanism of S-shaped behavior [9–11]. Ibtissem Fraj, et al reported that the S-shaped form in temperature-dependent PL peak energy of $In_{0.21}Ga_{0.79}As$ QW was attributed to carrier localization and polarization-induced electric fields on optical properties. For polar $In_{0.21}Ga_{0.79}As$ QW, the PL peak energy transferred from redshift to blueshift at a critical temperature. The temperature was demonstrated to be the equivalent point of localized and delocalized recombination processes. The higher the critical temperature was, the more thermal activation energies of photon-generated carriers hopping from band edges to localization centers were needed [12]. S. A. Lourenco, et al indicated that the negative thermal expansion (NTE) in $Al_xGa_{1-x}As$ alloy induced a small blueshift in the optical transition energy in the low temperature interval [13]. V. K. Dixit demonstrated that, under different experimental conditions, the domination of free carriers thermalization or localized carriers recombination led to the anomalous behaviors of PL energy and FWHM [14]. Torsten Langer, et al proposed that, an energy-dependent competition between radiative and nonradiative recombination processes, which was driven by an energy dependence of radiative lifetimes caused by piezoelectric fields, induced the 10 meV blue shift for polar GaInN/GaN QW [15]. As a quaternary compound with complex crystalline structure and complicated temperature response, AlGaInAs QWs exhibit more remarkable S-type low temperature response on optical properties than binary and ternary alloy systems [16].

In our previous work, we have investigated the defect evolution in thermally treated AlGaInAs QWs by spatially resolved cathodoluminescence (SRCL) [17]. In this paper, we attempted to study the mechanism of temperature-dependent PL peak energy of AlGaInAs QWs. A highly linear relationship between PL emission energy and FWHM of AlGaInAs QWs was demonstrated. It is indicated that, the mechanism at low temperature is a combination of strong carriers' localization and lattice strain fluctuations due to the difference of thermal

* Corresponding authors.
E-mail addresses: zhanglg@ciomp.ac.cn (L. Zhang), zengyg@ciomp.ac.cn (Y. Zeng).

https://doi.org/10.1016/j.materresbull.2019.02.027
Received 20 August 2018; Received in revised form 18 February 2019; Accepted 25 February 2019
Available online 01 April 2019
0025-5408/

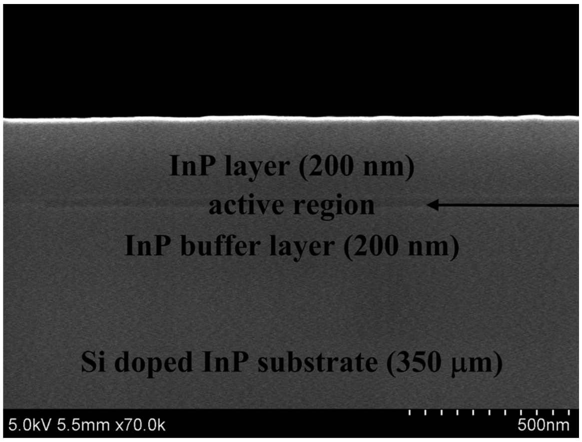

Fig. 1. The cross-sectional SEM of as-grown $Al_{0.07}Ga_{0.22}In_{0.71}As$ QW, and active layer (the arrow labelled) is composed of $Al_{0.225}Ga_{0.285}In_{0.49}As$ /$Al_{0.07}Ga_{0.22}In_{0.71}As$/$Al_{0.225}Ga_{0.285}In_{0.49}As$ QW.

expansion coefficients between adjacent layers.

2. Experimental

The $Al_{0.07}Ga_{0.22}In_{0.71}As$ QW was grown on a 350 μm thick, (001) Si-doped InP substrate by the AIXTRON 200/4 metal-organic chemical-vapor deposition (MOCVD) system. The active region was made up of a 6 nm $Al_{0.07}Ga_{0.22}In_{0.71}As$ quantum well sandwiched between two 10 nm $Al_{0.225}Ga_{0.285}In_{0.49}As$ barrier layers. The structural property of as-grown $Al_{0.07}Ga_{0.22}In_{0.71}As$ QW was characterized by cross-sectional scanning electron microscope (SEM), as represented in Fig. 1. The interfacial morphologies between epitaxial layers are quite well. The structure is the same as our previous work [17], which gave the detailed description of growth method and preparation process of AlGaInAs QW. The central region of the epitaxial wafer was cut into 15 pieces, 5 pieces of the samples were thermally treated at 170 °C for 2 h, and other 5 pieces were treated for 4 h. Heat treatment was carried out in a N_2 cover-gas environment. PL spectra were measured on a Jobin-Yvon Triax 550 spectrometer with 300 grooves per mm grating equipped by an InGaAs photodiode detector. The integration time was 0.1 s and scanning step-size increment was 1.0 nm in the experiment. The PL spectral resolution was 0.5 nm. These samples were placed in a cryogenic holder (ARS 8200 cryogenic system) which can adjust the temperature in range of 15–300 K and were excited by an 808-nm line of the continuous-wave semiconductor laser diode with a fixed power excitation of 12.5 W/cm^2. The lattices characteristics of QWs were measured by the Bruker D8 Discover high-resolution X-ray diffraction (CuK_α 40 KeV, 30 mA).

3. Results and discussion

The as-grown $Al_{0.07}Ga_{0.22}In_{0.71}As$ strained QW (without heat treatment) was studied by high-resolution X-ray diffraction (HR-XRD). The dominated InP diffraction peak and QW's multi-order satellite peaks coincided well with the curve simulated by Bruker LEPTOS, indicating that the quality of as-grown AlGaInAs QW is pretty good. The structural properties of samples annealed at 170 ℃ for 2 and 4 h were also investigated, and the diffraction patterns were quite similar to that of the as-grown sample, but the QW's multi-order satellite peaks moved to larger 2θ degrees a little. More details about the crystallization properties are performed in our recent work [17].

The band gap and interfacial potential of semiconductor materials are sensitive to temperature, which could be well reflected by temperature-dependent PL. Fig. 2 shows the PL spectra of $Al_{0.07}Ga_{0.22}In_{0.71}As$ QWs, as grown and thermally treated at 170 °C for 2 and 4 h over a temperature range from 15 to 300 K. For sample at a certain temperature, only a single emission band was observed, which exhibited an asymmetric line shape with a trailing edge superposing on the high energy side. The PL integral intensity increased obviously and the PL peak shifted simultaneously towards higher energy side when temperature was adjusted from 300 to 55 K. The PL intensity reached to a maximum at about 55 K. Generally speaking, PL intensity is strongly relevant to the density of photon-generated carriers which are related to the probability of carriers capture and escape from the QW layer. The increase of PL intensity can be explained by the decrement of photon-generated carriers' thermal escape from QW layer when temperature is lowering [18]. With temperature continued to decline, an obvious decrease in PL intensity occurred in all samples. The origin of the anomalous decreasing tendency of PL intensity in the temperature range from 55 to 35 K was associated with the drifting carriers decrement because of the carrier mobility decrease [19]. Additionally, the energy of PL peak shifted sharply to lower energy, the reason of the energy shift would be discussed in detail below.

Fig. 3 shows the temperature dependence of PL peak energy and FWHM of $Al_{0.07}Ga_{0.22}In_{0.71}As$ QWs with different thermal treatment durations at 170 °C. The PL peak energy was identified by the location of energy corresponding to the maximum of PL emission intensity, not from the line-shape fitting due to the asymmetric spectral line shape. An anomalous band-gap evolution, as S-shaped (decrease-increase-decrease) temperature-dependent PL peak energy was observed at low temperature. The S-shaped form in PL peak emission is rather similar to that reported in GaInNAs/GaAs [20] and InGaP material systems [21]. While the temperature was elevated from 15 to 40 K, the emission peak energy shifted towards lower energy, resulting in about 3.6, 3.92, 3.91 meV redshifts for $Al_{0.07}Ga_{0.22}In_{0.71}As$ QWs thermally treated at 170 °C for 0, 2, 4 h, respectively. Following on, the peak energy shifted sharply towards higher energy and reached maximum at about 55 K. The blue shifts of emission energy for $Al_{0.07}Ga_{0.22}In_{0.71}As$ QWs annealed at 170 °C for 0, 2, 4 h were 12.96, 4.58, 11.17 meV, respectively. In the high temperature region (> 55 K), the emission peak energy exhibited redshifts which could be well fitted by the Varshni semi-empirical formula (shown as dashed blue line in Fig. 3) [22]. However, the Varshni semi-empirical formula was impossible to simulate the experimental data at lower temperature range (T < 55 K).

Defects in band tail states could capture photon-generated carriers resulting in strong carrier localization in group III-V materials under lower temperature [8]. P. G. Eliseev, et al proposed a model based on the Varshni semi-empirical equation, which is amended by band-tail-state (BTS) to fit the experimental data, and Eq. (1) as followed [23].

$$Eg(T) = Eg(0) - \frac{\alpha T^2}{\beta + T} - \frac{\delta^2}{K_B T} \quad (1)$$

Where *Eg (0)* is the band gap at 0 K, α and β are the parameters for Varshni equation. K_B is the Boltzmann constant and δ is the band-tailing-state Gaussian broadening parameter of localized state. Each of the specific parameter values was calculated by linear interpolation method of corresponding value in binary and ternary systems. The optimizing parameter *Eg(0)*, α, β and δ from the best fit of $Al_{0.07}Ga_{0.22}In_{0.71}As$ QWs, as grown, thermally treated at 170 ℃ for 2 and 4 h were listed in Table 1 below. As shown in Fig. 3, it fitted quite well in the temperature region between 40 and 300 K (drawn in short-dashed red line).

Thus, the blue-shift could be understood in terms of that: carriers are trapped in low energy localized states at low temperature, and it is difficult for the trapped carriers to escape from the local potential. However, with temperature elevating, a competition between localized and delocalized recombination processes become noticeable. The increase of temperature promotes carriers to be thermally activated and redistribute to other strongly localized states via hopping [24]. As the redistribution effect is saturated, the enhancement of blue-shift in

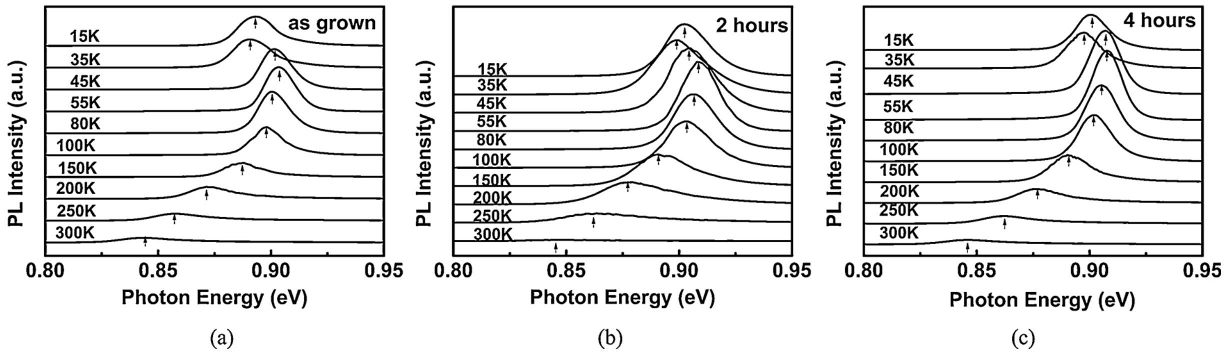

Fig. 2. PL spectra of $Al_{0.07}Ga_{0.22}In_{0.71}As$ QWs (a) as grown (b) thermally treated at 170 °C for 2 h (c) 4 h, respectively.

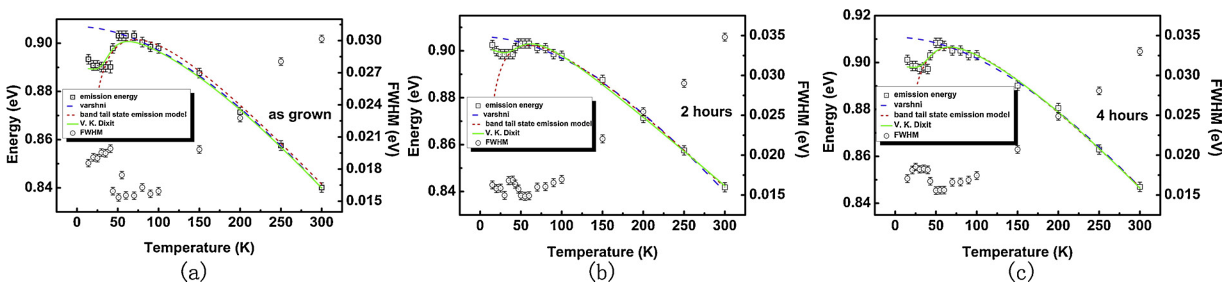

Fig. 3. Emission energy and FWHM of $Al_{0.07}Ga_{0.22}In_{0.71}As$ QWs thermally treated at 170 °C for (a) 0, (b) 2, (c) 4 h as a function of temperature. The varnish fitting curves are drawn in dashed blue line. The fitting curves of BTS model are drawn in short-dashed red line. The fitting curves of versatile phenomenological model proposed by V. K. Dixit are drawn in solid green line (For interpretation of the references to colour in this figure legend, the reader is referred to the web version of this article).

Table 1
Parameters obtained by analyzing the temperature-dependent PL data based on the band-tail-state (BTS) emission and versatile phenomenological model of AlGaInAs QWs thermal treated with different durations.

Model Name	Parameters	as grown	2 hours	4 hours
BTS emission model	*Eg(0) (eV)*	0.929	0.921	0.930
	α (eV/K)	3.9×10^{-4}	3.6×10^{-4}	3.7×10^{-4}
	β (K)	121	121	121
	δ	10.26	7.68	9.36
V. K. Dixit model	*Eg(0) (eV)*	0.912	0.913	0.916
	ΔE (meV)	21.3	12.9	17.8
	α (eV/K)	5.04×10^{-4}	4.8×10^{-4}	4.76×10^{-4}
	β (K)	323.578	322.61	317.33

optical transition energy is observed [25]. In the high temperature range (> 55 K), the red shift is caused by temperature-induced band gap shrinkage with carriers' thermal activation and delocalization due to electron-phonon interaction [26].

However, the empirical models mentioned above have some limitations, they are impossible to describe the temperature dependence of band gap in AlGaInAs QWs below 40 K. The versatile phenomenological model proposed by V. K. Dixit was demonstrated to be able to replicate the S-shaped behavior in many binary and ternary III-V semiconductor materials [14]. He proposed that the S-shaped behavior could be understood as whether carriers were captured by localized states or thermally activated under different testing environment. Eqs. (2–5) are given below.

$$E_{PL}^{peak} = (1-p)E_g(0) + pE_b - \frac{\alpha T^2}{\beta + T} \tag{2}$$

$$\Delta E = E_g(0) - E_b \tag{3}$$

$$P = \frac{1}{1 + \gamma \exp^{(\frac{-\Delta E}{K_B T})}} \tag{4}$$

$$E_{PL}^{peak} = E_g(0) - \frac{\Delta E}{1 + \gamma \exp^{(\frac{-\Delta E}{K_B T})}} - \frac{\alpha T^2}{\beta + T} \tag{5}$$

Where $E_g(0)$ is the delocalized state energy, E_b is the energy of localized state, p implies that band-to-band/localized state transition dominates the PL process, respectively, γ is a parameter related to the fitting model, K_B is the Boltzmann constant, ΔE represents the energy interval of the localized state from the delocalized state. The values of fitting parameters obtained by the versatile phenomenological model are also listed in Table 1 below.

As can be seen in Fig. 3, the changing trends of the simulation results obtained by the versatile phenomenological model proposed by V. K. Dixit (drawn in solid green line) match with that of the experimental data. However, our experimental data shows noticeable rising trend below 40 K, unlike the smooth simulation results. Moreover, we observed a steep dropping from 45 to 40 K which was impossible to be theoretically simulated [14].

In the experiment, all samples showed the same turning point from red shift to blue shift appeared in the vicinity of 40 K. This temperature was demonstrated to be the equivalent point between localization and delocalization recombination processes. Carriers diffuse from band edges to the localization centers and redistribute until this critical temperature [12]. The higher the critical temperature is, the more thermal activation energies of photon-generated carriers hopping from band edges to localization states are needed. Samples with different annealing durations showed the same critical temperature. Therefore, the thermal activation energies of photon-generated carriers hopping from the band edges to localized states were independent of annealing durations.

The FWHM was defined by the energy difference between the half-height of maximum peak intensity in each spectrum. FWHM evolution with temperature exhibited the identical tendency for three kinds of samples, shown in Fig. 3. They exhibited reverse temperature-dependent relationship in comparison with PL peak energy. The FWHM increased slowly with temperature rising up to 40 K. In the temperature range of 40 to 55 K, the PL line-width decreased sharply, which was opposite to the traditional broadening due to the exciton-photon coupling. Finally, the PL line-width increased as the temperature was raised in range of 55–300 K, which is in accordance with most semiconductor bulk [27]. In general, the FWHM of PL emission spectrum is made up of two parts (inhomogeneous and homogenous broadening terms). The inhomogeneous broadening term is determined by the fluctuations of circumstance, such as composition variation, interface roughness and strain potential [28,29]. But it is independent of measured environment. The homogeneous term is significantly influenced by the interaction between electrons and phonons. At low temperature (below 40 K), the FWHM is mainly determined by inhomogeneous broadening, and its evolution is affected by lattice strain fluctuations due to the difference of thermal expansion coefficients between adjacent layers led by composition variation, *etc* [30]. In the temperature range, most carriers are localized in the band-tail states and localized states. With temperature increasing to the critical temperature, carriers possess enough thermal energy enabling their delocalization. The reduction of FWHM ranging from 40 to 55 K is due to the de-trapping process. Above 55 K, the increment of PL line-width was assumed as a combination between carriers' thermalization and phonon scattering due to the enhancement of temperature [31].

FWHM evolution vs the corresponding emission central energy for each sample in the experimental temperature range is plotted in Fig. 4, and the temperature covers the whole region from 15 to 300 K. A negative linear relationship between them could be observed. The fitted linearity curve was obtained by using least-squares method plotted as black solid line in Fig. 4. Although the evolutions of QW emission peak energy and FWHM in the low temperature region were quite different from that of the high temperature region, the linear relationship indicated that the evolutions of the QW emission peak energy and FWHM with temperature obeyed the same or associated mechanism. The slope were -0.25, -0.31 and -0.29 for samples as grown, thermally treated for 2 and 4 h respectively, suggesting that the coupling of carriers and the surrounding environment in $Al_{0.07}Ga_{0.22}In_{0.71}As$ QWs were slightly different. The variation of PL peak energy vs temperature in the low temperature range was affected by carriers' localization, and the FWHM was relevant to the fluctuations of circumstance. Based on the highly linear relationship, the mechanism of temperature-dependent PL peak energy and FWHM is a combination of strong carriers' localization and lattice strain fluctuations due to the difference of thermal expansion coefficients between adjacent layers.

Fig. 5 zoomed up the temperature-dependent PL peak energy of $Al_{0.07}Ga_{0.22}In_{0.71}As$ QWs, as grown and annealed at 170 °C for 2 h in the temperature range from 15 to 70 K. As can be seen, a sharp drop in PL peak energy in the vicinity of 45 K and a rising up below 40 K were exhibited. However, the fitting curve was quite flat at the temperature range below 40 K. Thus the versatile phenomenological model proposed by V. K. Dixit could not well match the temperature-dependent PL peak energy evolution of quaternary AlGaInAs strained QWs. The model proposed that the energy interval of the localized state from the delocalized state (ΔE) is a certain constant. But in fact, the thermal expansion coefficient always non-linearly change with temperature in low temperature range [32]. As reported in literature, there is a valley transition in temperature-dependent thermal expansion coefficient of both InAs [33] and GaAs [34] at temperature about 35 to 45 K. The temperature-dependent thermal expansion coefficient of $Al_{0.07}Ga_{0.22}In_{0.71}As$ is able to be estimated by weighted superposition [35]. The thermal expansion coefficient of $Al_{0.07}Ga_{0.22}In_{0.71}As$ QW decreases with temperature lifting below 40 K, but increases with temperature while temperature is above 40 K. Especially for multilayer semiconductor structure, the stress led by the difference of thermal expansion coefficients between adjacent layers could strongly affect the level of delocalized and localized state. Hence, we attempted to employ thermal expansion effect and strain potential to interpret the variation of carrier transitions energy in this temperature range (T < 45 K).

For our multi-layer quaternary material system, the energy positions of localized state and delocalized state are significantly affected by the stress led by the difference of thermal expansion coefficients between adjacent layers. The energy interval of the localized state from the delocalized state is not a constant at low temperature, so we proposed that the deviation of versatile phenomenological model is attributed to the lattice strain fluctuations caused by thermal expansion coefficients difference.

4. Conclusions

The optical properties of quaternary $Al_{0.07}Ga_{0.22}In_{0.71}As$ QW have been investigated systematically by temperature dependence of PL spectroscopy. An S-shaped curve was observed in PL peak energy vs temperature relationship for differently thermal treated AlGaInAs QWs. The temperature dependence of PL peak energy and FWHM exhibited a reversed trend. A highly linear relationship between them indicated that the same or associated mechanism dominated their evolutions with temperature: the anomalous blue shift and concomitant narrowing of FWHM were attributed to lattice strain fluctuations due to difference of thermal expansion coefficients and strong carriers' localization. Each sample showed that the turn off point from red shift to blue shift appeared at 40 K, indicating that the thermal energies of photon-generated carriers moving from the band edges to localization centers were independent of annealing durations.

Acknowledgments

This work was financially supported by National Science and Technology Major Project of China (No. 2016YFE0126800), in part by National Natural Science Foundation of China (No. 11874353, 61727822, 51672264, 61434005, 61674148), in part by Program of equipment development of Chinese Academy of sciences (NO. YZ201560, YJKYYQ20180045), in part by the Science and Technology

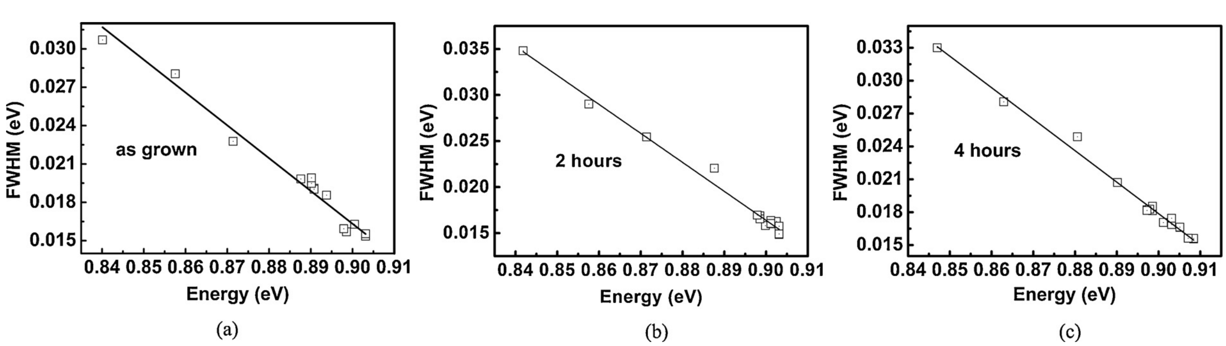

Fig. 4. The relationship between photon energy and FWHM for $Al_{0.07}Ga_{0.22}In_{0.71}As$ QWs (a) as grown, (b) annealed for 2 h (c) annealed for 4 h, respectively. The linear fit curves for as grown and annealed are drawn in black solid line.

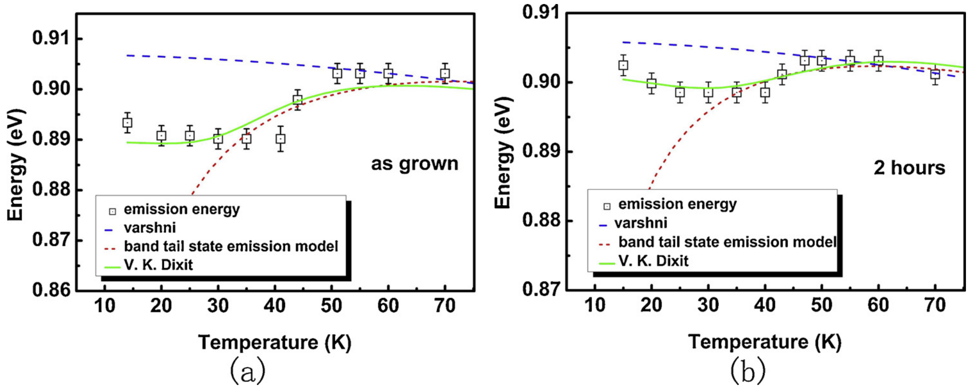

Fig. 5. Zoomed up of temperature-dependent PL peak energy of $Al_{0.07}Ga_{0.22}In_{0.71}As$ QWs, as grown and annealed at 170 ℃ for 2 h in the temperature range of.15–70 K.

Program of Jilin province (No. 20170204013GX), in part by the Frontier Science Key Program of President of the Chinese Academy of Sciences (No. QYZDY-SSW-JSC006), in part by Science and Technology Development Project of Jilin Province (No. 20160414016GH).

References

[1] O.J. Pitts, W. Benyon, A.J. Springthorpe, Modeling and process control of MOCVD growth of InAlGaAs MQW structures on InP, J. Cryst. Growth 393 (2014) 81–84, https://doi.org/10.1016/j.jcrysgro.2013.10.019.
[2] A. Caliman, A. Mereuta, G. Suruceanu, V. Iakovlev, A. Sirbu, E. Kapon, 8 mW fundamental mode output of wafer-fused VCSELs emitting in the 1550 nm band, Opt. Express 19 (2011) 16996–17001, https://doi.org/10.1364/OE.19.016996.
[3] J.D. Song, J.S. Yu, J.M. Kim, S.J. Bae, Y.T. Lee, Effects of rapid thermal annealing on the optical properties of 1.3 μm InGaAlAs multiquantum wells grown by digital-alloy molecular-beam epitaxy, J. Appl. Phys. 80 (2002) 4650–4652, https://doi.org/10.1063/1.1485132.
[4] A.A. Sirenko, A. Kazimirov, R. Huang, D.H. Bilderback, S. O'Malley, V. Gupta, K. Bacher, L.J.P. Ketelsen, A. Ougazzaden, Microbeam high-resolution x-ray diffraction in strained InGaAlAs-based multiple quantum well laser structures grown selectively on masked InP substrates, J. Appl. Phys. 97 (2005) 063512, , https://doi.org/10.1063/1.1862769g.
[5] T. Higashi, S.J. Sweeney, A.F. Phillips, A.R. Adams, E.P. O'Reilly, T. Uchida, T. Fujii, Experimental analysis of temperature dependence in 1.3-μm AlGaInAs-InP strained MQW lasers, IEEE J. Sel. Top. Quantum 5 (1999) 413–419, https://doi.org/10.1109/2944.788399.
[6] M.A. Pinault, E. Tournié, On the origin of carrier localization in $Ga_{1-x}In_xN_yAs_{1-y}$/GaAs quantum wells, Appl. Phys. Lett. 78 (2001) 1562–1564, https://doi.org/10.1063/1.1354153.
[7] P.G. Eliseev, M. Osinski, J. Lee, T. Sugahara, S. Sakai, Band-tail model and temperature-induced blue-shift in photoluminescence spectra of $In_xGa_{1-x}N$ grown on sapphire, J. Electron. Mater. 29 (2000) 332–341.
[8] T. Li, A.M. Fischer, Q.Y. Wei, F.A. Ponce, T. Detchprohm, C. Wetzel, Carrier localization and nonradiative recombination in yellow emitting InGaN quantum wells, Appl. Phys. Lett. 96 (2010) 031906, , https://doi.org/10.1063/1.3293298.
[9] X.L. Zhou, Y.H. Chen, J.Q. Liu, B. Xu, X.L. Ye, Z.G. Wang, Abnormal temperature dependent photoluminescence of self-assembled InAs/GaAs surface quantum dots with high areal density, Phys. E 42 (2010) 2455–2459, https://doi.org/10.1016/j.physe.2010.06.008.
[10] S. Shirakata, M. Kondow, T. Kitatani, Temperature-dependent photoluminescence of high-quality GaInNAs single quantum wells, Appl. Phys. Lett. 80 (2002) 2087–2089, https://doi.org/10.1063/1.1463208.
[11] Y.H. Cho, B.D. Little, G.H. Gainer, J.J. Song, S. Keller, U.K. Mishra, S.P. DenBaars, Carrier dynamics of abnormal temperature-dependent emission shift in mocvd-grown InGaN epilayers and InGaN/GaN quantum wells, Mat. Res. Symp. Proc. 537 (1998), https://doi.org/10.1557/S1092578300002271.
[12] I. Fraj, T. Hidouri, F. Saidi, L. Bouzaiene, L. Sfaxi, H. Maaref, Effect of carriers localized in clusters on optical properties of $In_{0.21}Ga_{0.79}As$/GaAs multiple quantum wells, Curr. Appl. Phys. 17 (2017) 1–5, https://doi.org/10.1016/j.cap.2016.10.013.
[13] S.A. Lourenço, I.F.L. Dias, J.L. Duarte, E. Laureto, L.C. Pocas, D.O. Toginho Filho, J.R. Leite, Thermal expansion contribution to the temperature dependence of excitonic transitions in GaAs and AlGaAs, Braz. J. Phys. 34 (2004) 517–525, https://doi.org/10.1590/S0103-97332004000300031.
[14] V.K. Dixit, S. Porwal, S.D. Singh, T.K. Sharma, S. Ghosh, S.M. Oak, A versatile phenomenological model for the S-shaped temperature dependence of photoluminescence energy for an accurate determination of the exciton localization energy in bulk and quantum well structures, J. Phys. D Appl. Phys. 47 (2014) 65103–65116, https://doi.org/10.1088/0022-3727/47/6/065103.
[15] T. Langer, H.G. Pietscher, F.A. Ketzer, H. Jönen, H. Bremers, U. Rossow, D. Menzel, A. Hangleiter, S shape in polar GaInN/GaN quantum wells: piezoelectric-field-induced blue shift driven by onset of nonradiative recombination, Phys. Rev. B 90 (2014) 205302, , https://doi.org/10.1103/PhysRevB.90.205302.
[16] A.A. Bernussi, H. Temkin, High temperature properties of quaternary quantum well laser diodes, Rev. Bras. Fisioter. 27 (1997) 29–37.
[17] Y. Song, L.G. Zhang, Y.G. Zeng, L. Qin, Y.L. Zhou, Y.Q. Ning, L.J. Wang, Microscopic view of defect evolution in thermal treated AlGaInAs quantum well revealed by spatially resolved cathodoluminescence, Materials 11 (2018) 1049, https://doi.org/10.3390/ma11061049.
[18] M. Kondo, N. Okada, K. Domen, K. Sugiura, C. Anayama, T. Tanahashi, Origin of nonradiative recombination centers in AlGaInP grown by metalorganic vapor phase epitaxy, J. Electron. Mater. 23 (1994) 355–358, https://doi.org/10.1007/BF03296064.
[19] Y.T. Fang, L. Wang, Q.L. Sun, T.P. Lu, Z. Deng, Z.G. Ma, Y. Jiang, H.Q. Jia, W.X. Wang, J.M. Zhou, H. Cheng, Investigation of temperature-dependent photoluminescence in multi-quantum wells, Sci. Rep. 5 (2015) 12718, https://doi.org/10.1038/srep12718.
[20] L. Grenouillet, C. Bru-Chevallier, G. Guillot, P. Gilet, P. Duvaut, C. Vannuffel, A. Million, A. Chenevas-Paule, Evidence of strong carrier localization below 100 K in a GaInNAs/GaAs single quantum well, Appl. Phys. Lett. 76 (2000) 2241–2243, https://doi.org/10.1063/1.126308.
[21] M. Kondow, S. Minagawa, Y. Inoue, T. Nishino, Y. Hamakawa, Anomalous temperature dependence of the ordered $Ga_{0.5}In_{0.5}P$ photoluminescence spectrum, Appl. Phys. Lett. 54 (1989) 1760–1762, https://doi.org/10.1063/1.101283.
[22] R. Pässler, Basic model relations for temperature dependencies of fundamental energy gaps in semiconductors, Phys. Stat. Sol. 200 (1997) 155–172, https://doi.org/10.1002/1521-3951(199703)200:1 < 155::AID-PSSB155 > 3.0.CO;2-3.
[23] P.G. Eliseev, The red σ^2/kT spectral shift in partially disordered semiconductors, J. Appl. Phys. 93 (2003) 5404–5415, https://doi.org/10.1063/1.1567055.
[24] D. Watson-Parris, M.J. Godfrey, P. Dawson, R.A. Oliver, M.J. Galtrey, M.J. Kappers, C.J. Humphreys, Carrier localization mechanisms in $In_xGa_{1-x}N$/GaN quantum wells, Phys. Rev. B 3 (2011) 1409–1413, https://doi.org/10.1103/PhysRevB.83.115321.
[25] I. Fraj, F. Saidi, L. Bouzaiene, L. Sfaxi, H. Maref, Piezoelectric field effect on the optical properties of $In_{0.21}Ga_{0.79}As$/GaAs (113) MQW, Opt. Mater. 58 (2016) 121–127, https://doi.org/10.1016/j.optmat.2016.05.021.
[26] N. Sarkar, S. Ghosh, The temperature dependence of the band gap shrinkage due to the electron phonon interaction in $Al_xGa_{1-x}As$, J. Phys-Condens. Mat. 18 (2006) 1687–1694, https://doi.org/10.1088/0953-8984/18/5/021.
[27] M.K. Bafna, P. Sen, P.K. Sen, Temperature dependence of the photoluminescence properties of self-assembled InGaAs/GaAs single quantum dot, J. Appl. Phys. 100 (2006) 103515, , https://doi.org/10.1063/1.2387054.
[28] T. Zhu, E. Ertekin, Resolving anomalous strain effects on two-dimensional phonon flows: the cases of graphene, boron nitride, and planar superlattices, Phys. Rev. B 91 (2015) 205429, , https://doi.org/10.1103/PhysRevB.91.205429.
[29] D. Vashaee, A. Shakouri. Electronic and thermoelectric transport in semiconductor and metallic superlattices, J. Appl. Phys. 95 (2004) 1233–1245, https://doi.org/10.1063/1.1635992.
[30] L.G. Zhang, D.Z. Shen, X.W. Fan, S.Z. Lv, Exciton-phonon scattering in CdSe/ZnSe quantum dots, Chin. Phys. Lett. 19 (2002) 578–580 http://cpl.iphy.ac.cn/Y2002/V19/I4/0578.
[31] T. Unuma, M. Yoshita, T. Noda, H. Sakaki, H. Akiyama, Intersubband absorption linewidth in GaAs quantum wells due to scattering by interface roughness, phonons, alloy disorder, and impurities, J. Appl. Phys. 93 (2003) 1586–1597, https://doi.org/10.1063/1.1535733.
[32] V.M. Glazov, A.S. Pashinkin, Thermal expansion and heat capacity of GaAs and InAs, Inorg. Mater. 36 (2000) 225–231, https://doi.org/10.1007/BF02757926.
[33] P.W. Sparks, C.A. Swenson, Thermal expansions from 2 to 40°K of Ge, Si and four III-V Compounds, Phys. Rev. 163 (1967) 779–790, https://doi.org/10.1103/PhysRev.163.779.
[34] T. Soma, J. Satoh, H. Matsuo, Thermal expansion coefficient of GaAs and InP, Solid State Commun. 42 (1982) 889–892, https://doi.org/10.1016/0038-1098(82)90233-2.
[35] J.K. Burton, S.L. Phoenix, Superposition method for calculating singular stress fields at kinks, branches and tips in multiple crack arrays, Int. J. Fract. 102 (2000) 99–139, https://doi.org/10.1023/A:1007558018808.